



# Nonlinear dynamics of a nonsmooth shape memory alloy oscillator

Bruno Cardozo dos Santos, Marcelo Amorim Savi \*

*Universidade Federal do Rio de Janeiro, COPPE, Department of Mechanical Engineering, 21.941.972,  
P.O. Box 68.503, Rio de Janeiro, RJ, Brazil*

Accepted 16 July 2007

---

## Abstract

In the last years, there is an increasing interest in nonsmooth system dynamics motivated by different applications including rotor dynamics, oil drilling and machining. Besides, shape memory alloys (SMAs) have been used in various applications exploring their high dissipation capacity related to their hysteretic behavior. This contribution investigates the nonlinear dynamics of shape memory alloy nonsmooth systems considering a linear oscillator with a discontinuous support built with an SMA element. A constitutive model developed by Paiva et al. [Paiva A, Savi MA, Braga AMB, Pacheco PMCL. A constitutive model for shape memory alloys considering tensile-compressive asymmetry and plasticity. *Int J Solids Struct* 2005;42(11–12):3439–57] is employed to describe the thermomechanical behavior of the SMA element. Numerical investigations show results where the SMA discontinuous support can dramatically change the system dynamics when compared to those associated with a linear elastic support system. A parametric study is of concern showing the system behavior for different system characteristics, forcing excitation and also gaps. These results show that smart materials can be employed in different kinds of mechanical systems exploring some of the remarkable properties of these alloys.

© 2007 Elsevier Ltd. All rights reserved.

---

## 1. Introduction

Smart materials are being used in different fields of human knowledge. Shape memory alloys (SMAs) are included in this class of materials and, among other characteristics, are easy to manufacture, relatively lightweight, and able of producing high forces or displacements with low power consumption. There are many applications related to SMA devices including seals, connectors and clamps [13,22]. Self-actuating fasteners, thermally actuator switches and several bioengineering devices are other important examples of applications [3,7,9,10]. Besides, the high dissipation capacity of these alloys has been employed in order to introduce a smart dissipation in system dynamics.

On the other hand, nonsmooth systems appear in many kinds of engineering systems and also in everyday life [5]. Examples may be mentioned by the stick-slip oscillations of a violin string or grating brakes. Moreover, it is related to some related phenomena as chatter and squeal that cause serious problems in many industrial applications. Nonsmooth

---

\* Corresponding author. Tel.: +55 21 2562 8372; fax: +55 21 2562 8383.  
E-mail address: [savi@mecanica.ufrj.br](mailto:savi@mecanica.ufrj.br) (M.A. Savi).

systems have been analyzed in order to understand various engineering problems: Oil drilling [4,16,24], rotor dynamics [6] and machining [23] are some interesting examples. Nonsmooth nonlinearity is usually associated with either the friction phenomenon or the discontinuous characteristics as intermittent contacts of some system components.

The objective of this research effort is to investigate the use of SMA in nonsmooth systems exploring its high dissipation capacity. This is done by considering a single degree of freedom oscillator with discontinuous support. This device is previously addressed in [2,19] where an elastic support is treated by numerical and experimental approaches. In this contribution, the elastic discontinuous support is replaced by an SMA element and it is investigated its influence in system dynamics. Since hysteretic response of shape memory alloys is one of their essential characteristics, its description is essential for the correct system comprehension. The thermomechanical description of SMA is done employing a constitutive model that assumes four macroscopic phases and different material properties for each phase. This constitutive model presents close agreement with experimental data being capable to capture the general thermomechanical behavior of SMAs including internal sub-loops [14,15,20].

A predictor–corrector numerical scheme is employed together with an iterative process in order to deal with the system nonlinearities. Therefore, it is assumed an operator split technique [11], and the fourth order Runge–Kutta method is used together with the orthogonal projection algorithm. Numerical investigation is carried out showing comparisons between the system dynamics with linear elastic and SMA supports identifying the main aspects related to the SMA behavior. These results show situations where the SMA discontinuous support dramatically change the system dynamics when compared to those associated with a linear elastic support.

## 2. Constitutive model

There are different ways to describe the thermomechanical behavior of SMAs [14]. Here, a constitutive model that is built upon the Fremond's model and previously presented in references [1,14,15,21] is employed. This model considers different material properties to each phase and four macroscopic phases for the description of the SMA behavior. The tension–compression asymmetry, the plastic strain and the plastic-phase transformation coupling are incorporated in the original model. Nevertheless, for the sake of simplicity, these characteristics are not considered in this article and, moreover, only two martensitic phases may be induced. Therefore, the thermomechanical behavior of SMA is described by the following set of equations:

$$\sigma = E\varepsilon - [E\alpha_h + \alpha]\beta - \Omega(T - T_0) \quad (1)$$

$$\dot{\beta} = \frac{1}{\eta} \{ \alpha\varepsilon + A(T) + (2\alpha\alpha_h + E\alpha_h^2)\beta + \alpha_h[E\varepsilon - \Omega(T - T_0)] - \partial_{\beta} J_{\pi} \} + \partial_{\beta} J_{\chi} \quad (2)$$

$$\dot{\beta}_A = \frac{1}{\eta_A} \left\{ -\frac{1}{2}(E_A - E_M)[\varepsilon + \alpha_h\beta]^2 + A_A(T) + (\Omega_A - \Omega_M)(T - T_0)[\varepsilon + \alpha_h\beta] - \partial_{\beta_A} J_{\pi} \right\} + \partial_{\beta_A} J_{\chi} \quad (3)$$

Here  $\varepsilon$  is the strain,  $T$  is the temperature,  $\beta$  is the volumetric fraction of detwinned martensite,  $\beta_A$  represents the volumetric fraction of the austenite. Moreover,  $E = E_M + \beta_A(E_A - E_M)$  is the elastic modulus while  $\Omega = \Omega_M + \beta_A(\Omega_A - \Omega_M)$  is related to the thermal expansion coefficient. Notice that subscript A refers to austenitic phase, while M refers to martensite. Parameters  $A = A(T)$  and  $A_A = A_A(T)$  are associated with phase transformation stress levels. Parameter  $\alpha_h$  is introduced in order to define the horizontal width of the stress–strain hysteresis loop, while  $\alpha$  controls the vertical width of the hysteresis loop on stress–strain diagrams.

The terms  $\partial_n J_{\pi}$  ( $n = \beta, \beta_A$ ) are sub-differentials of the indicator function  $J_{\pi}$  with respect to  $n$ . This indicator function is related to a convex set  $\pi$ , which provides the internal constraints related to the phases' coexistence. With respect to evolution equations of volumetric fractions,  $\eta$  and  $\eta_A$  represent the internal dissipation related to phase transformations. Moreover  $\partial_n J_{\chi}$  ( $n = \beta, \beta_A$ ) are sub-differentials of the indicator function  $J_{\chi}$  with respect to  $n$ . This indicator function is associated with the convex set  $\chi$ , which establishes conditions for the correct description of internal sub-loops due to incomplete phase transformations. These sub-differentials may be replaced by Lagrange multipliers associated with the mentioned constraints [21].

Concerning parameter definitions, linear temperature dependent relations are adopted for  $A$  and  $A_A$  as follows:

$$A = -L_0 + \frac{L}{T_M}(T - T_M) \quad A_A = -L_0^A + \frac{L^A}{T_M}(T - T_M) \quad (4)$$

Here  $T_M$  is the temperature below which the martensitic phase becomes stable. Besides,  $L_0$ ,  $L$ ,  $L_0^A$  and  $L^A$  are parameters related to critical stress for phase transformation.

In order to contemplate different characteristics of the phase transformation kinetics for loading and unloading processes, it is possible to consider different values to the parameters  $\eta$  and  $\eta_A$ :  $\eta^L$  and  $\eta_A^L$  during loading while  $\eta^U$  and  $\eta_A^U$  are used during unloading process. For more details about the constitutive model see [15,20].

### 3. Oscillator with discontinuous support

The dynamical response of a single-degree of freedom system with an SMA discontinuous support, shown in Fig. 1, is analyzed in this contribution. The oscillator is composed by a mass  $m$  connected by two linear springs with stiffness  $k$ . Dissipation process may be modeled by a linear damping with coefficient  $c$ . Moreover, the support is massless, having a linear damping with coefficient  $c_s$  and also an element that could be either linear elastic or made by SMA. The mass displacement is denoted by  $x$ , relative to the equilibrium position and the distance between the mass and the support is defined by a gap  $g$ . The support displacement is denoted by  $e$ . Therefore, the system has two possible modes, represented by a situation where the mass presents contact with the support and other situation when there is no contact. Calling  $f_s$  as the contact force between the mass and the support, these two situations may be represented as follows [8,19]:

$$\begin{cases} x < g & \text{and } f_s = 0, & \text{without contact} \\ x \geq g & \text{and } f_s = -(K + c_s \dot{x}) < 0, & \text{with contact} \end{cases} \quad (5)$$

where  $K = K(e) = K(x - g)$  represents the restitution force of the support element. By assuming an SMA support, its thermomechanical behavior needs to be evaluated from a proper constitutive equation as presented in the previous section. This element may be either a spring or a bar and, in both cases, it is possible to establish a relation between the force–displacement and the stress–strain curves [12,18]. In general, one assumes that  $K = B\sigma$ . Notice that, if  $\sigma$  represents a bar axial stress,  $B$  represents the bar cross sectional area. On the other hand, if  $\sigma$  is related to a shear stress,  $B$  should be a parameter evaluated from a helical spring characteristics. Moreover, it should be highlighted that the restitution force may be assumed to be linear,  $K = k_s e = k_s(x - g)$ , representing a linear elastic element.

According to these conditions, it is written the following equations of motion:

$$\begin{cases} m\ddot{x} + 2kx + c\dot{x} = \rho \cos(\omega t), & \text{without contact} \\ m\ddot{x} + 2kx + K + (c + c_s)\dot{x} = \rho \cos(\omega t), & \text{with contact} \end{cases} \quad (6)$$

This system is representative of the dynamical behavior of different applications. For instance, it may be understood as a one-dimensional version of the rotor dynamics problem discussed in [6] and a variation of the oil drilling problem discussed in [4,16,24].

A numerical procedure based on the operator split technique is employed in order to deal with the system nonlinearities. Basically, it is assumed a predictor–corrector scheme together with an iterative process. Under this assumption, the equations of motion become uncoupled allowing the use of classical procedures to solve the problem. In this article, the fourth order Runge–Kutta method is employed to estimate the variables dynamical evolution assuming that phase transformation does not take place. A switch model is used in order to consider the change between contact and non-contact situations. Afterwards, the constitutive model is solved considering the procedure developed in [21]. This process is repeated until a prescribed tolerance is assured.

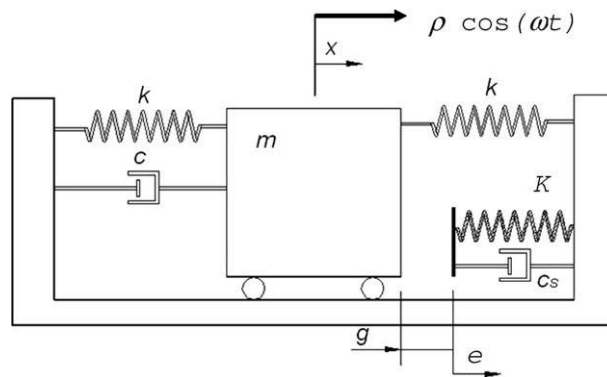


Fig. 1. Nonsmooth system with discontinuous support.

#### 4. Numerical simulations

Numerical simulations regarding the nonlinear dynamics of a single degree of freedom oscillator with discontinuous support are of concern. Two different situations are treated: linear elastic support and SMA support. In order to allow a comparison between results predicted by both models, it is assumed the same oscillator characteristics and also an SMA support with the same austenitic elastic response than the linear elastic support. Table 1 presents the SMA constitutive parameters. Under this condition, it is possible to evaluate the main effects related to the phase transformations in SMA response. This section considers a parametric analysis investigating the effect of different parameter variations. Basically, it is investigated the influence of system dissipation, forcing parameters (frequency and amplitude) and gap.

All simulations consider the following oscillator parameters:  $m = 0.838$  kg and  $k = 8.47$  N/m. Moreover, the support parameters are:  $k_s = 1350$  N/m (elastic support) and  $B = 2.5 \times 10^{-8}$  m<sup>2</sup> (SMA support). Other parameters are varied depending on the analysis.

##### 4.1. Dissipation effects

The nonlinear dynamics analysis of the oscillator with discontinuous support starts considering the effect of system dissipation represented by the linear viscous damping. It is assumed  $c_s = 0.6$  N s/m,  $g = -0.0045$  m and forcing parameters  $\rho = 4.5$  N and  $\omega = 2.3$  rad/s. In order to obtain a global understanding of the system behavior, bifurcation diagrams are presented showing the stroboscopic sample of state variables (displacement and velocity) under the slow quasi-static variation of dissipation parameter  $c$ . Linear elastic and SMA support system responses are plotted together in Fig. 2. The elastic support system presents a complex behavior, presenting chaotic-like response for low values of dissipation parameter. The more this parameter is increased, the less complex is the system response. On the other hand, the response of the system with SMA support dissipates energy enough to obtain a less complex behavior for all dissipation parameters.

Table 1  
SMA constitutive parameters

| $E_A$ (GPa)        | $E_M$ (GPa)        | $\alpha$ (MPa)     | $\varepsilon_R$    |
|--------------------|--------------------|--------------------|--------------------|
| 54                 | 42                 | 150                | 0.055              |
| $L_0$              | $L$                | $L_0^A$            | $L^A$              |
| 0.15               | 4                  | 6.3                | 165                |
| $\Omega_A$ (MPa/K) | $\Omega_M$ (MPa/K) | $T_M$ (K)          | $T_0$ (K)          |
| 0.74               | 0.17               | 291.4              | 298                |
| $\eta^L$ (MPa s)   | $\eta^U$ (MPa s)   | $\eta_A^L$ (MPa s) | $\eta_A^U$ (MPa s) |
| 8                  | 2                  | 5                  | 5                  |

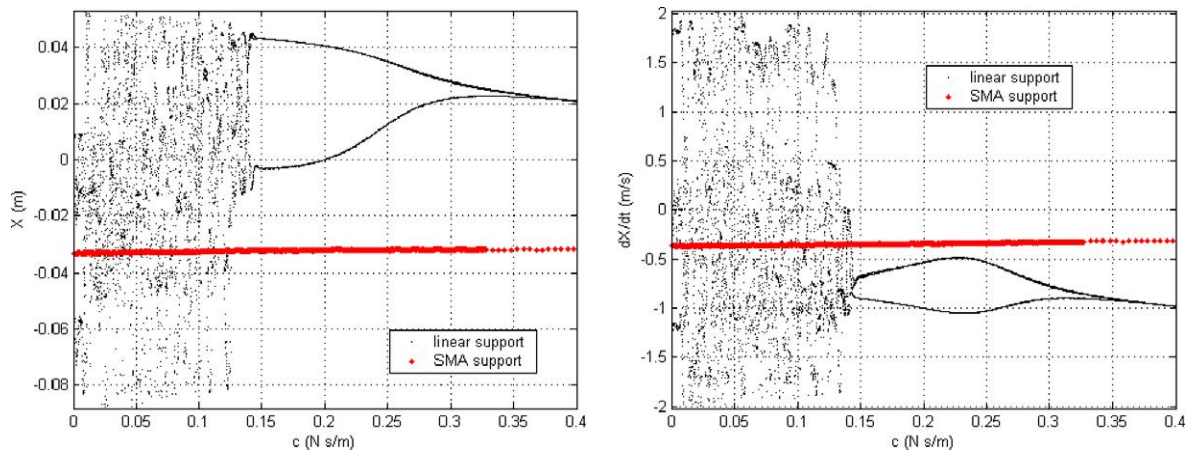


Fig. 2. Bifurcation diagram varying dissipation parameter.

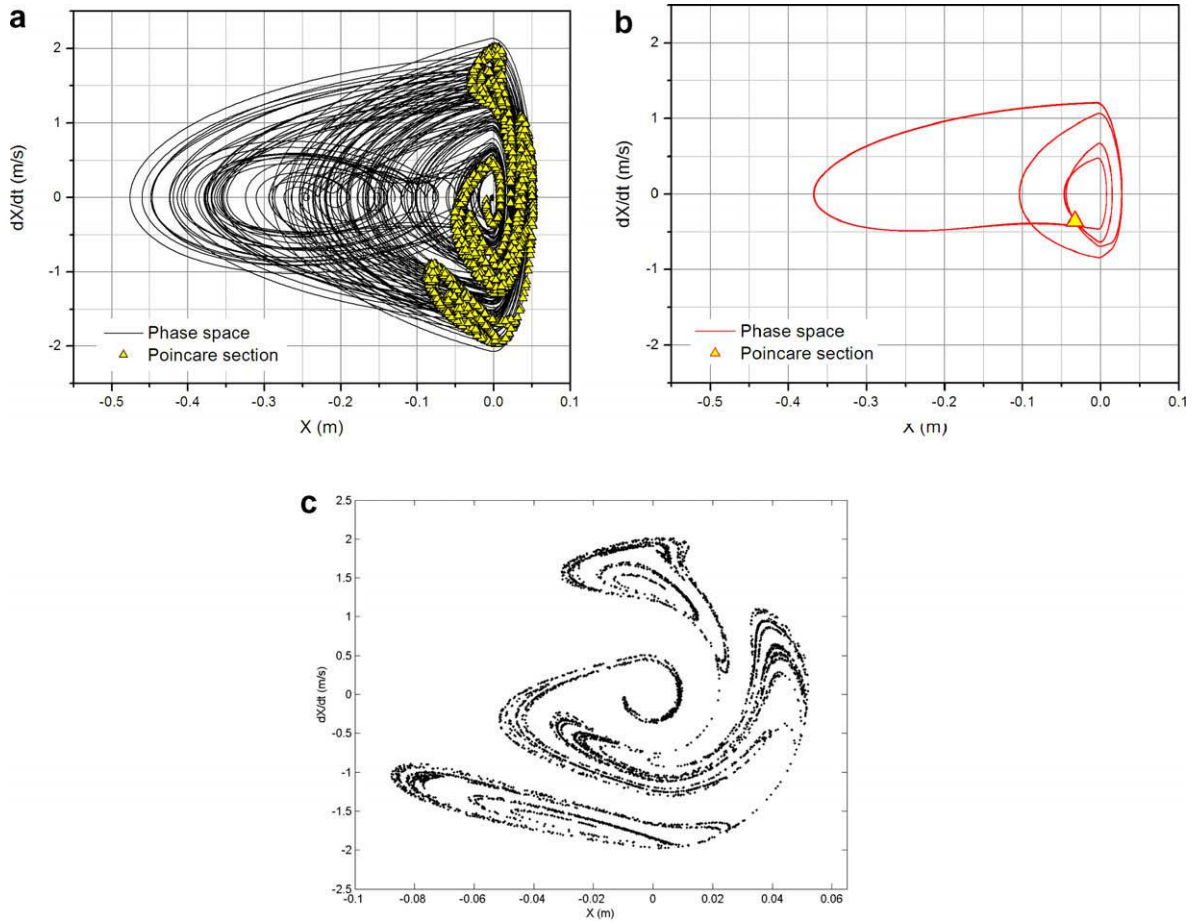


Fig. 3. Systems response for  $c = 0.05$  N/m/s. (a) Linear support model. (b) SMA support model, (c) Poincaré section with linear support.

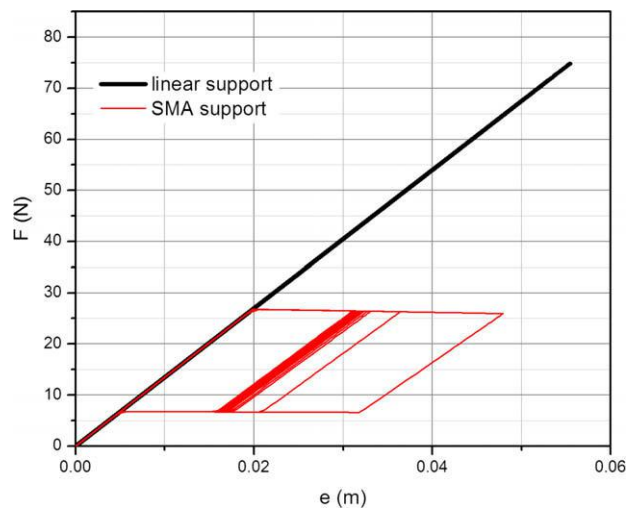


Fig. 4. Force–displacement curve for  $c = 0.05$  N/m/s.

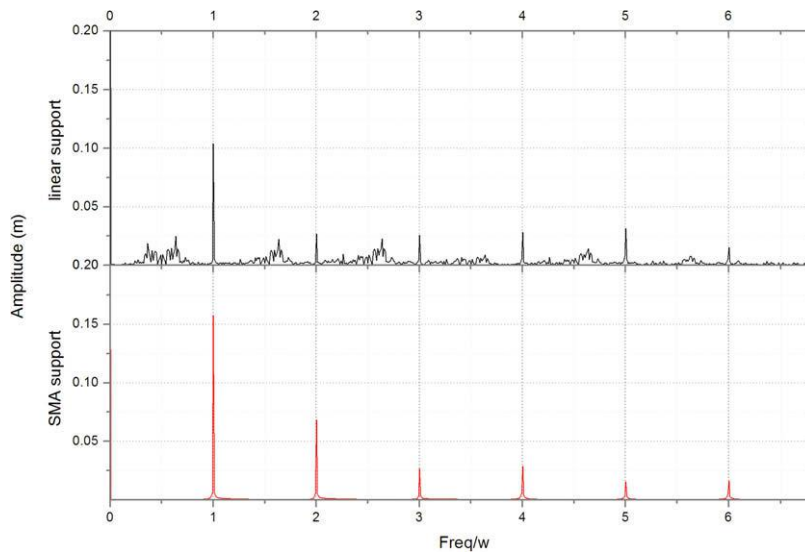


Fig. 5. Frequency spectrum response for  $c = 0.05$  N m/s.

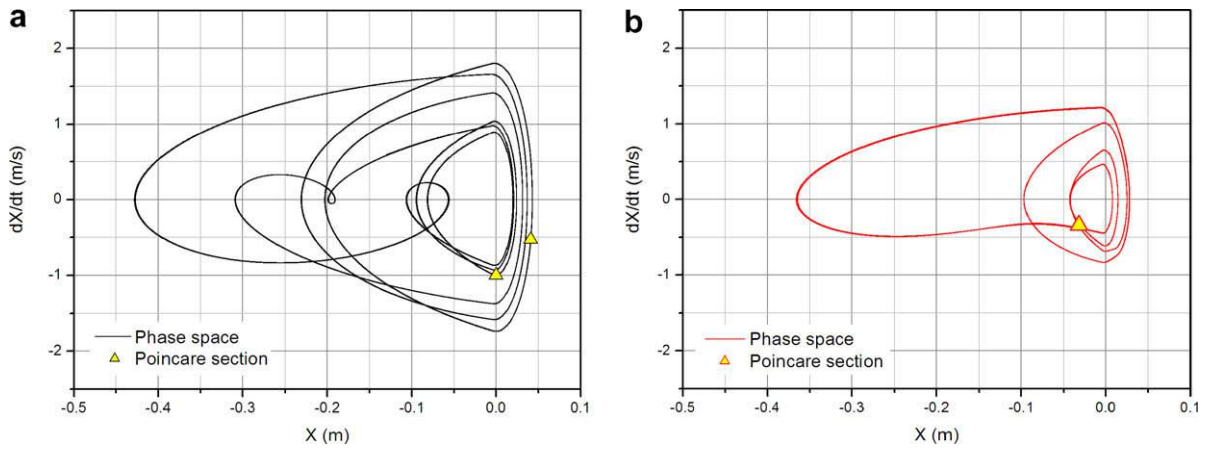


Fig. 6. System response for  $c = 0.2$  N m/s. (a) Linear support model, (b) SMA support model.

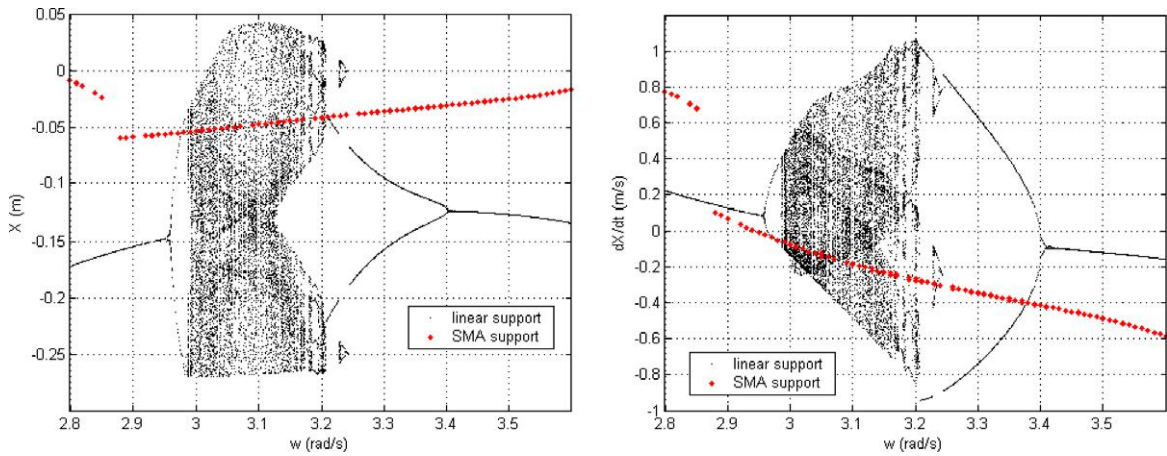


Fig. 7. Bifurcation diagrams varying amplitude frequency.

Different dissipation parameter values are now in focus in order to show some system response characteristics. Fig. 3 shows the system response for  $c = 0.05$  N m/s, a value inside the cloud of points in bifurcation diagram. Under this condition, the elastic support system response is chaotic-like, presenting a strange attractor with fractal-like structure. On the other hand, the SMA support system presents a periodic response. This difference is explained by the high dissipation capacity of the SMA system due to hysteresis loop. Fig. 4 presents the force–displacement curves of both sup-

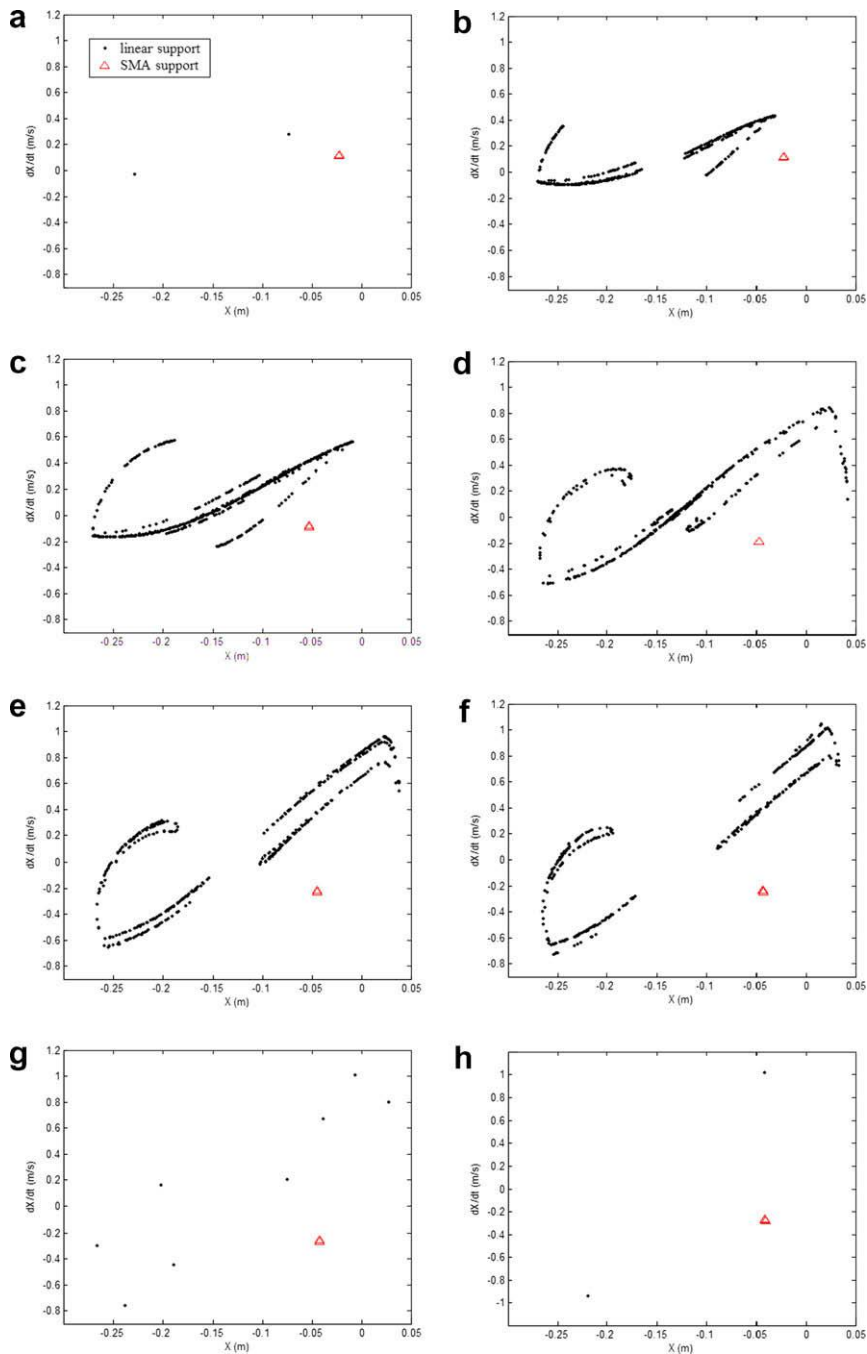


Fig. 8. Sequence of Poincaré sections for different frequency values. (a)  $\omega = 2.97$  rad/s, (b)  $\omega = 2.99$  rad/s, (c)  $\omega = 3.01$  rad/s, (d)  $\omega = 3.11$  rad/s, (e)  $\omega = 3.15$  rad/s, (f)  $\omega = 3.17$  rad/s, (g)  $\omega = 3.19$  rad/s (h)  $\omega = 3.21$  rad/s.

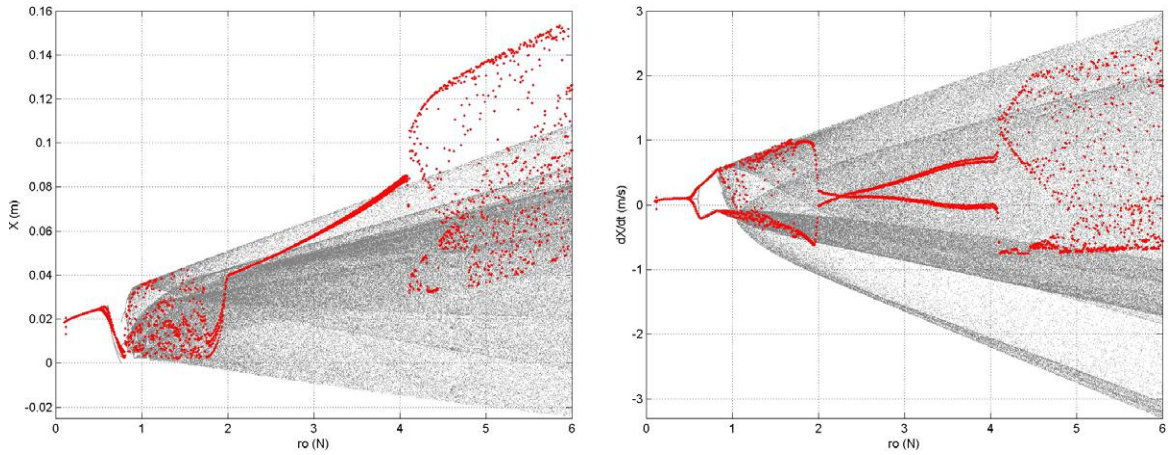


Fig. 9. Bifurcation diagram varying the forcing amplitude.

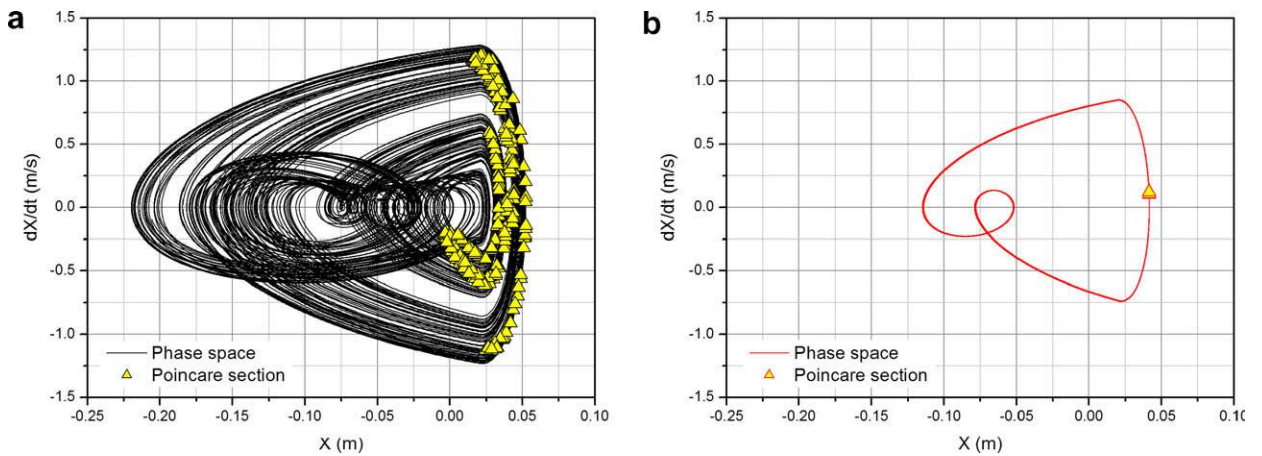


Fig. 10. System response for  $\rho = 2.1$  N. (a) Linear support model, (b) SMA support model.

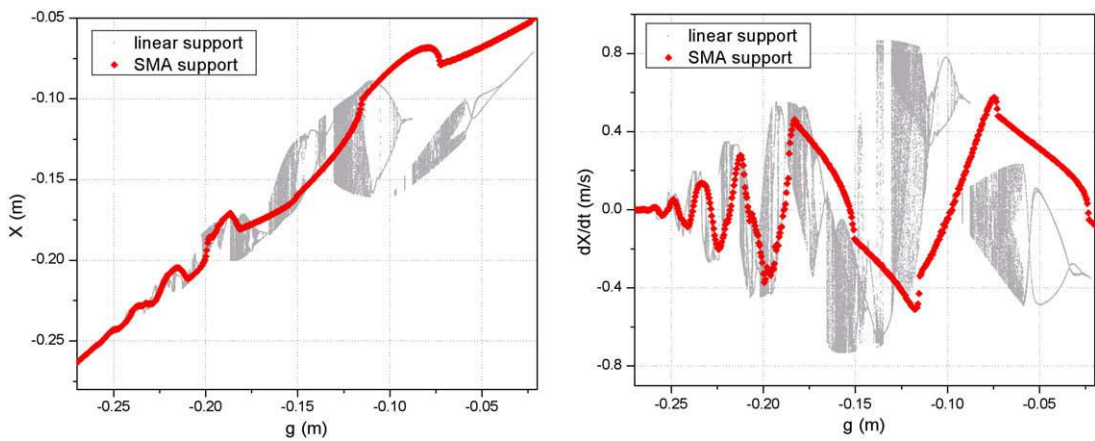


Fig. 11. Bifurcation diagram varying the gap.

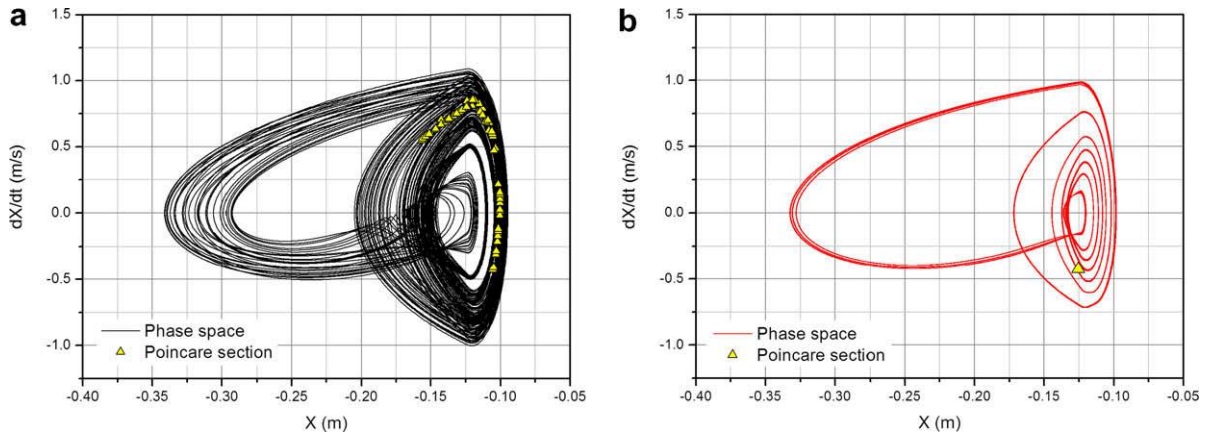


Fig. 12. System response for  $g = -0.124$  m. (a) Linear support model, (b) SMA support model.

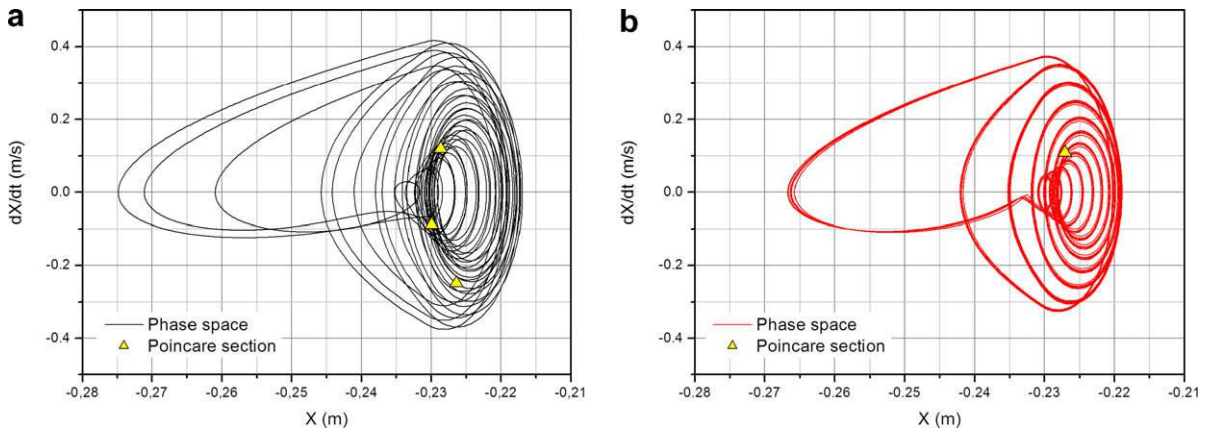


Fig. 13. System response for  $g = -0.2307$  m. (a) Linear support model, (b) SMA support model.

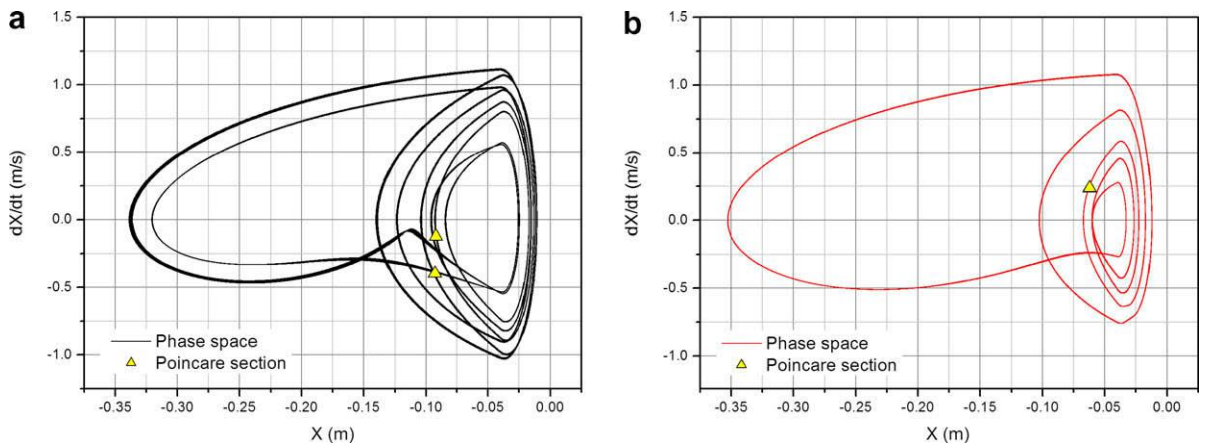


Fig. 14. System response for  $g = -0.04$  m. (a) Linear support model, (b) SMA support model.

ports during the transient response. The SMA hysteresis loop dissipates an amount of energy that eliminates the chaotic response of the elastic system. By observing the frequency spectrum (Fig. 5) it is also noticeable that the energy is spread over a wider bandwidth in the elastic support system response.

At this point, a different dissipation parameter is analyzed ( $c = 0.2 \text{ N m/s}$ ). This value is again related to a more complex behavior of the linear elastic support when compared with the behavior of the SMA support system (Fig. 6).

It should be highlighted that the SMA support introduces dissipation to the system, dramatically changing its response when compared to that obtained from the linear elastic support system. Notice that the dissipation increase of the linear elastic support system, which is done by changing the dissipation parameter, tends to homogenize both system behaviors.

#### 4.2. Forcing characteristic effects

The forcing characteristics effects are now in focus. It is assumed  $c = 0.3 \text{ N s/m}$ ,  $c_s = 0.6 \text{ N s/m}$ ,  $g = 0.02 \text{ m}$ . Bifurcation diagrams are presented showing the stroboscopic sample of state variables (displacement and velocity) under the slow quasi-static variation of forcing parameters. Forcing frequency is analyzed first assuming  $\rho = 4.5 \text{ N}$ . Linear elastic and SMA support system responses are plotted together in Fig. 7. Once again, the high dissipative behavior of SMA support tends to produce less complex behaviors when compared to those from the elastic support system. Fig. 8 presents a sequence of Poincare sections for different frequency values showing the system response evolution. The mentioned difference between elastic and SMA support responses is clear noticeable.

The same kind of behavior obtained from the forcing frequency analysis may be expected concerning the forcing amplitude effect. Fig. 9 presents the bifurcation diagram associated with this parameter, assuming  $\omega = 4.5 \text{ rad/s}$ . For low amplitude values, both systems present the same behavior since SMA hysteresis loop is not reached. The increase of this amplitude, however, tends to change the system response. Fig. 10 presents the response of both systems for  $\rho = 2.1 \text{ N}$ . Notice that linear elastic support system response is chaotic-like while the SMA support response is periodic.

#### 4.3. Gap effects

The parametric study now contemplates the gap influence on the discontinuous support oscillator nonlinear dynamics. Now, it is assumed  $c = 0.87 \text{ N s/m}$ ,  $c_s = 0.6 \text{ N s/m}$  and forcing parameters  $\rho = 4.5 \text{ N}$  and  $\omega = 2.3 \text{ rad/s}$ . The analysis is started by presenting bifurcation diagrams changing the gap parameter. Linear elastic and SMA support system responses are plotted together in Fig. 11. The elastic support system has complex behaviors, presenting bifurcations and chaos as the gap changes. Once again, the energy dissipation related to the SMA system causes less complex behaviors for all gap parameter.

Different gap values are now in focus in order to compare results of both systems. At first,  $g = -0.124 \text{ m}$  is considered (Fig. 12). Under this condition, elastic support system presents a chaotic-like response while SMA support system has a period-1 response. By changing the gap for  $g = -0.2307 \text{ m}$  (Fig. 13), elastic support system presents a periodic

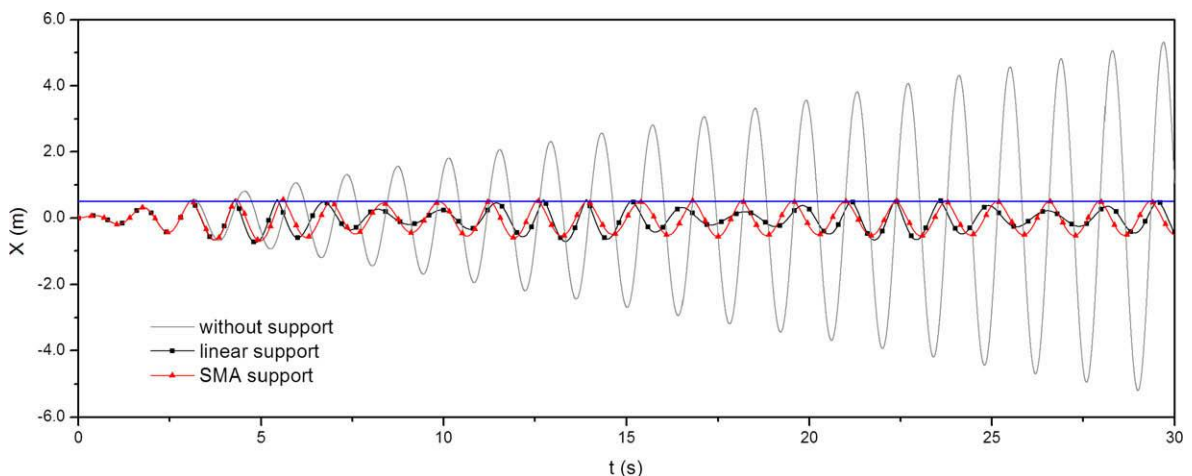


Fig. 15. Comparisons among system response under linear resonant conditions.

response while the SMA support system has a qualitative similar response. Assuming  $g = -0.04$  m (Fig. 14), both systems have periodic responses showing that less complex behaviors are expected as a consequence of the reducing of negative gaps.

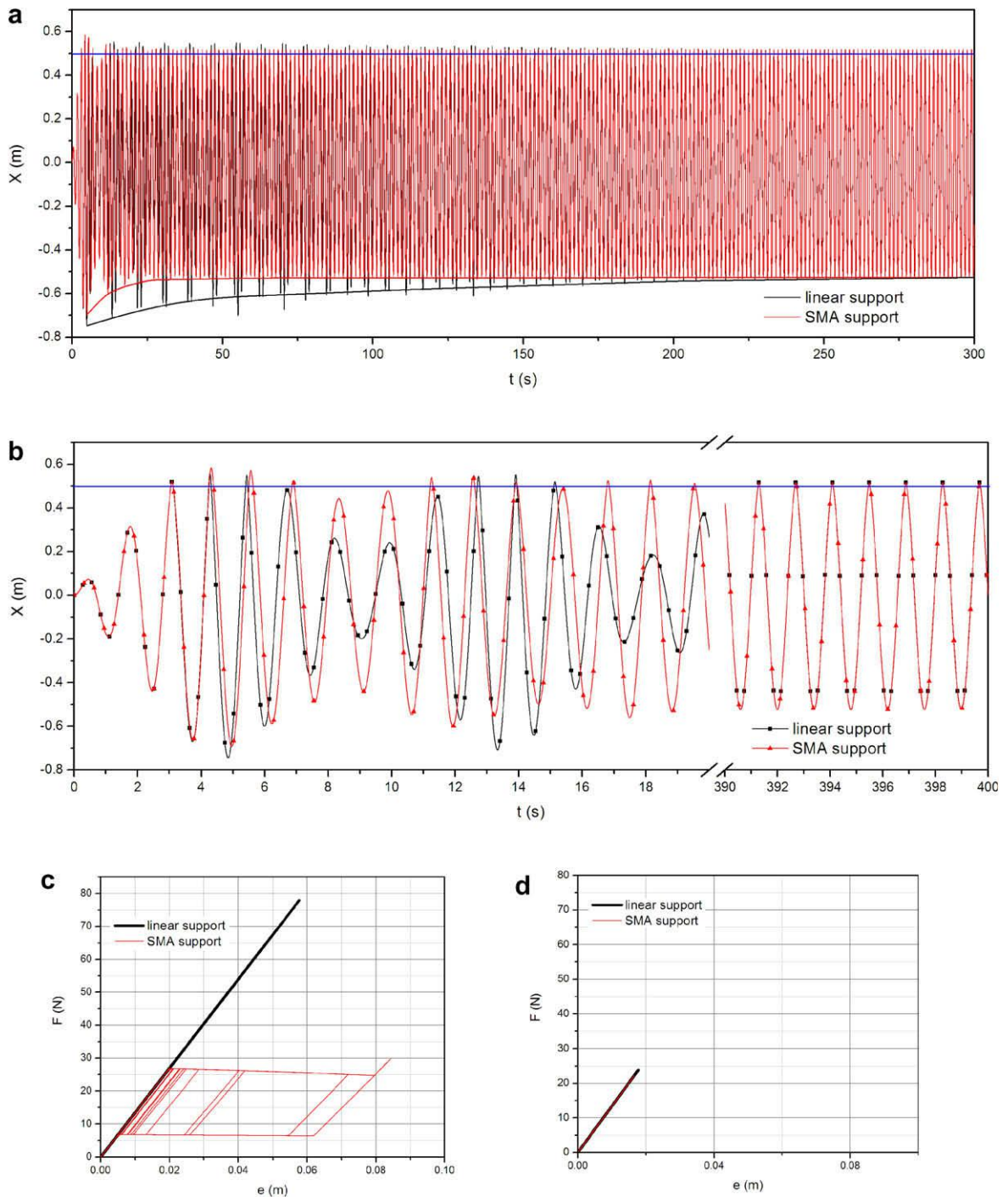


Fig. 16. System response under linear resonant conditions: (a) time histories; (b) transient and steady state regimes (c) Support response under transient regime, (d) Support response under steady state regime.

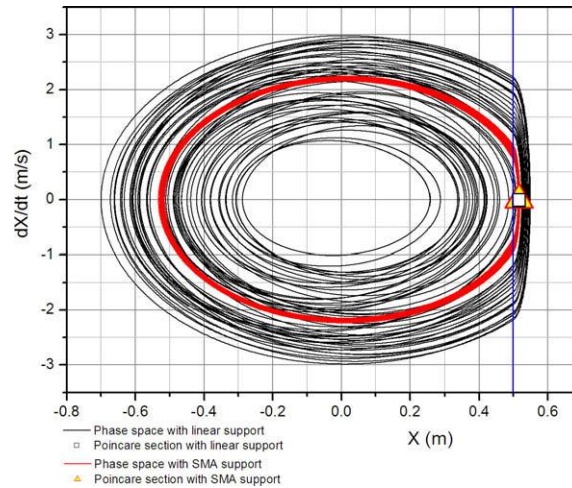


Fig. 17. System response under linear resonant conditions.

#### 4.4. Support effects under resonant conditions

At this point, it is considered an important situation in terms of engineering purposes: the use of the high dissipation capacity of SMA support in order to avoid undesirable behaviors associated with resonant conditions. In order to analyze this phenomenon, the following parameters are considered:  $c = 0$ ,  $c_s = 0.6$  N s/m  $g = 0.5$  m and forcing parameters  $\rho = 1.35$  N and  $\omega = 4.5$  rad/s. As it is well-known, a non-dissipative linear oscillator under resonant conditions tends to indefinitely increase its amplitude. The introduction of the linear elastic support tends to dissipate system energy, changing this kind of behavior. On the other hand, the SMA support also dissipates energy but in a more efficient way when compared with the elastic support system. Fig. 15 presents a comparison among these three kinds of responses. Either the linear elastic support system or the SMA support system presents the same steady state response, as it is shown in Fig. 16, however, the SMA response has a smaller transient. Fig. 16 shows the force–displacement curves showing that the difference between transient responses is due to the energy dissipated by the SMA hysteresis loop. Fig. 17 shows the steady state response of the SMA support system and the elastic support system for the same period of time, which is related to a transient response.

## 5. Conclusions

This contribution discusses the nonlinear dynamics response of a single degree of freedom oscillator with a discontinuous SMA support. The thermomechanical behavior of the SMA is described by a constitutive model proposed by Paiva et al. [15]. Results of this system are compared with those obtained considering a linear elastic support. A parametric analysis is carried out considering the effects of system dissipation, forcing characteristics and gap. Moreover, it is shown the effect of the SMA support in order to avoid undesirable effects under resonant conditions. In general, it is possible to conclude that the high dissipation capacity of SMA due to the hysteresis loop is capable to produce less complex behaviors, dramatically changing the system response when compared to those obtained from the linear elastic support system. Concerning engineering applications, it should be noticed that SMA support can be imagined as passive vibration control avoiding inconvenient transients during starting and stopping of machines. Besides, SMA support may avoid some kinds of bifurcations, simplifying dynamical system response and allowing the energy use in a desirable frequency.

## Acknowledgement

The author acknowledges the support of Brazilian Research Council (CNPq).

## References

- [1] Baêta-Neves AP, Savi MA, Pacheco PMCL. On the Fremond's constitutive model for shape memory alloys. *Mech Res Commun* 2004;31(6):677–88.
- [2] Divenyi S, Savi MA, Franca LFP, Weber HI. Nonlinear dynamics and chaos in systems with discontinuous support. *Shock Vibr* 2006;13(4/5):315–26.
- [3] Duerig TM, Pelton A, Stöckel D. An overview of nitinol medical applications. *Mater Sci Eng A* 1999;273–275:149–60.
- [4] Franca LFP, Weber HI. Experimental and numerical study of a new resonance hammer drilling model with drift. *Chaos, Solitons & Fractals* 2004;21:789–801.
- [5] Hinrichs N, Oestreich M, Popp K. On the modelling of friction oscillators. *J Sound Vibr* 1998;216(3):435–59.
- [6] Karpenko EV, Pavlovskaja EE, Wiercigroch M. Bifurcation analysis of a preloaded Jeffcott rotor. *Chaos, Solitons & Fractals* 2003;15:407–16.
- [7] Lagoudas DC, Rediniotis OK, Khan MM. Applications of shape memory alloys to bioengineering and biomedical technology. In: *Proceedings of fourth international workshop on mathematical methods in scattering theory and biomedical technology*; 1999.
- [8] Leine RI. Bifurcations in discontinuous mechanical systems of Filippov-type. PhD thesis, Technische Universiteit Eindhoven; 2000.
- [9] Machado LG, Savi MA. Medical applications of shape memory alloys. *Braz J Med Biol Res* 2003;36(6):683–91.
- [10] Machado LG, Savi MA. Odontological applications of shape memory alloys. *Revista Bras Odontol* 2002;59(5):302–6 [in Portuguese].
- [11] Ortiz M, Pinsky PM, Taylor RL. Operator Split Methods for the Numerical Solution of the Elastoplastic Dynamic Problem. *Comput Methods Appl Mech Eng* 1983;39:137–57.
- [12] Pacheco PMCL, Savi MA, Paiva A. Phenomenological modeling of shape memory alloy helical spring. In: *COBEM 2007 – 19th international congress of mechanical engineering*; 2007.
- [13] Pacheco PMCL, Savi MA. Modeling and simulation of a shape memory release device for aerospace applications. *Revista de Engenharia e Ciências Aplicadas*; 2000.
- [14] Paiva A, Savi MA. An overview of constitutive models for shape memory alloys. *Mathematical problems in engineering*, v.2006, Article ID56876; 2006. p. 1–30.
- [15] Paiva A, Savi MA, Braga AMB, Pacheco PMCL. A Constitutive Model for Shape Memory Alloys Considering Tensile-Compressive Asymmetry and Plasticity. *Int J Solids Struct* 2005;42(11–12):3439–57.
- [16] Pavlovskaja E, Wiercigroch M, Grebogi C. Modeling of an impact system with a drift. *Phys Rev E* 2001;64:056224.
- [18] Savi MA, Sa MAN, Paiva A, Pacheco PMCL. Tensile-compressive asymmetry influence on the shape memory alloy system dynamics. *Chaos, Solitons & Fractals* 2008;36(4):828–42.
- [19] Savi MA, Divenyi S, Franca LFP, Weber HI. Numerical and experimental investigations of the nonlinear dynamics and chaos in non-smooth systems. *J Sound Vibr* 2007;301(1–2):59–73.
- [20] Savi MA, Paiva A. Describing internal subloops due to incomplete phase transformations in shape memory alloys. *Arch Appl Mech* 2005;74(9):637–47.
- [21] Savi MA, Paiva A, Baêta-Neves AP, Pacheco PMCL. Phenomenological Modeling and Numerical Simulation of Shape Memory Alloys: A Thermo-Plastic-Phase Transformation Coupled Model. *J Intell Mater Syst Struct* 2002;13(5):261–73.
- [22] van Humbeeck J. Non-medical Applications of Shape Memory Alloys. *Mater Sci Eng A* 1999;273–275:134–48.
- [23] Warminski J, Litak G, Cartmell MP, Khanin R, Wiercigroch M. Approximate analytical solutions for primary chatter in the non-linear metal cutting model. *J Sound Vibr* 2003;259(4):917–33.
- [24] Wiercigroch M, Wojewoda J, Krivtsov AM. Dynamics of ultrasonic percussive drilling of hard rocks. *J Sound Vibr* 2005;280(3–5): 739–57.